NASA TECHNICAL MEMORANDUM

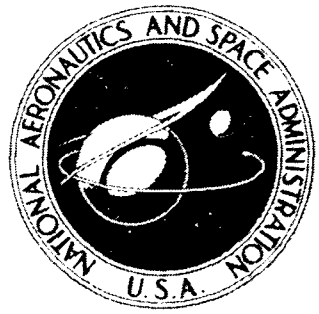

NASA TM X-2736

NASA TM X-2736

DETERMINATION AND EVALUATION OF PERFORMANCE LIMIT CRITERIA OF FAST-RESPONSE ELECTROHYDRAULIC SERVOSYSTEMS

by John R. Zeller and John A. Webb, Jr.

Lewis Research Center
Cleveland, Ohio 44135

NATIONAL AERONAUTICS AND SPACE ADMINISTRATION • WASHINGTON, D. C. • MARCH 1973

1. Report No.	2. Government Accession No.	3. Recipient's Catalog No.
NASA TM X-2736		

4. Title and Subtitle	5. Report Date
DETERMINATION AND EVALUATION OF PERFORMANCE LIMIT CRITERIA OF FAST-RESPONSE ELECTROHYDRAULIC SERVOSYSTEMS	March 1973
	6. Performing Organization Code

7. Author(s)	8. Performing Organization Report No.
John R. Zeller and John A. Webb, Jr.	E-7239
	10. Work Unit No. 501-24

9. Performing Organization Name and Address	11. Contract or Grant No.
Lewis Research Center National Aeronautics and Space Administration Cleveland, Ohio 44135	
	13. Type of Report and Period Covered
12. Sponsoring Agency Name and Address	Technical Memorandum
National Aeronautics and Space Administration Washington, D.C. 20546	14. Sponsoring Agency Code

15. Supplementary Notes

16. Abstract

Limit criteria for determining the dynamic performance capabilities of high-performance, fast-response (>100 Hz) electrohydraulic servosystems are presented. A detailed analysis of the maximum load locus of these systems is used as a basis for the derivation of improved limit criteria. These criteria predict the maximum performance limits caused by system nonlinearities and physical limitations. The criteria are applied to experimental data to verify their validity. Design criteria which assist in the selection of system components for optimal performance are also discussed.

17. Key Words (Suggested by Author(s))	18. Distribution Statement
Servosystems Electrohydraulic serosystems Fast response systems	Unclassified - unlimited

19. Security Classif. (of this report)	20. Security Classif. (of this page)	21. No. of Pages	22. Price*
Unclassified	Unclassified	29	$3.00

* For sale by the National Technical Information Service, Springfield, Virginia 22151

DETERMINATION AND EVALUATION OF PERFORMANCE LIMIT CRITERIA OF FAST-RESPONSE ELECTROHYDRAULIC SERVOSYSTEMS

by John R. Zeller and John A. Webb, Jr.

Lewis Research Center

SUMMARY

Advanced propulsion system research has dictated a significant need for high-performance, fast-response (>100 Hz) servosystems. The two-stage electrohydraulic servovalve and piston-in-cylinder actuator used for this purpose has a high-frequency response which is dependent upon certain physical limits of the hydraulic actuating components. The maximum region of dynamic performance can be determined by considering these physical limitations and component nonlinearities.

A detailed analysis of the maximum load locus of these systems is presented as a basis for the derivation of improved limit criteria. The criteria are applied to electrohydraulic servosystem data to verify their validity. A design criterion which assists in the selection of system components is derived as an extension to the limit criteria. The maximum region of dynamic performance is presented in normalized form based on optimum performance.

INTRODUCTION

Research activities in the area of advanced propulsion systems have dictated a significant need for high-performance, fast-response (>100 Hz) servosystems. This need is twofold: first, as disturbance devices for studying the high-frequency dynamics of propulsion systems and components; and second, as a control loop element for complex systems.

The type of equipment normally selected to provide this fast-response control capability is the two-stage electrohydraulic servovalve and piston-in-cylinder actuator arrangement. Its basic closed-loop configuration is shown in figure 1. The equipment is well suited to this application for several reasons. First, it has the inherent capa-

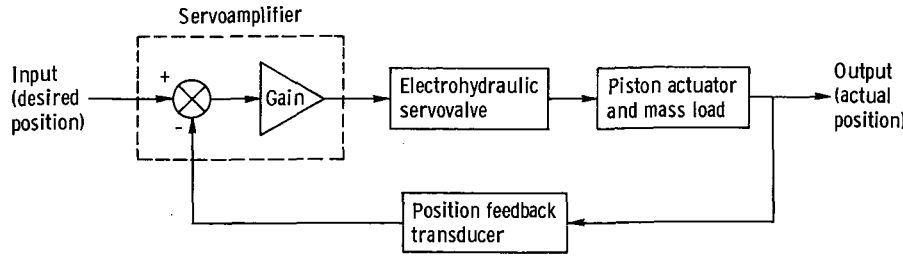

Figure 1. - Basic closed-loop configuration of electrohydraulic servosystem.

bility of modulating large amounts of energy at the desired high-frequency rates. Second, most propulsion system manipulated variables can be arranged in a configuration that adapts well to the linear motion of piston-in-cylinder actuators. Finally, the electrical input nature of the system makes it suitable for accepting well defined input waveforms and thus greatly simplifies the subsequent task of interpreting research performance data. Sinusoidal motion of the output load is a typical disturbance used for studying transient performance through the use of frequency response techniques.

In many applications employing this control system configuration, the natural hydraulic resonant frequency of the actuator and load combination will limit the range of dynamic performance (ref. 1). In this report, the systems which are to be manipulated at these high rates of response (>100 Hz), however, involve relatively small mass loads. Thus, by hydraulically closely coupling the servovalve and piston actuator to minimize the entrapped volume of hydraulic fluid, the hydraulic spring-load mass resonant frequency can be made to occur well beyond the dynamic performance range of interest.

Elimination of this natural performance limitation puts the closely coupled, low-mass electrohydraulic servosystems into a somewhat specialized category. The dynamic performance capabilities of the higher frequency systems now become quite dependent upon certain physical limits of the hydraulic power actuating components. The magnitude and frequency of sinusoidal output performance will be bounded as a function of certain of these limitations. The region within this boundary will be the maximum region of dynamic performance capability.

Reference 2 presents an analysis of nonlinear component limitations and predicts the performance boundary for a specific servosystem configuration. Additional experience with propulsion system servosystems has indicated that some of the somewhat arbitrary assumptions used to arrive at the limit criteria of reference 2 were too conservative. This prompted a derivation of an elliptical load line (locus) which permitted sinusoidal output motion of sufficient size to pass through the peak power transfer point of the servovalve. From this less conservative load locus a new set of limit criteria can be derived which have a firm analytical basis.

This report presents the derivation of the peak power transfer load line for inertial loads, the subsequent derivation of a new set of performance limit criteria, and an application of the limit criteria to an electrohydraulic servosystem used for propulsion research. It is intended that the presentation will be detailed enough to demonstrate the value of a nonlinear analysis in evaluating systems with high-performance requirements. The analysis also will establish a normalized design criterion based on those component limitations found to be significant.

DESCRIPTION OF OUTPUT OPERATION

It is desired to evaluate this specialized class of electrohydraulic servosystems for sinusoidal operation of the actuator output shaft position $x_o(t)$. This operation can be described as follows:

$$x_o(t) = X_o \sin \omega t \tag{1}$$

$$\dot{x}_o(t) = X_o \omega \cos \omega t \tag{2}$$

$$\ddot{x}_o(t) = -X_o \omega^2 \sin \omega t \tag{3}$$

(Symbols are defined in appendix A.) The component limitations of the electrohydraulic power actuating components of the servosystem limit the range of peak displacements X_o and frequencies ω over which the system can operate. A description of the components is presented in the next section so that relations defining the region of X_o and ω over which a servosystem may be capable of operating can be derived.

ANALYTICAL DESCRIPTION OF POWER ACTUATING COMPONENTS

Load and Piston Actuator Force Balance

For the category of systems under consideration, the load being actuated by a double-ended cylinder is assumed to have negligible friction and spring (position-dependent) types of loading. Also, it is assumed to have no opposing forces. When the notation of figure 2 is used, the following equations result:

$$p_p(t)A_p = M_o\ddot{x}_o(t) \tag{4}$$

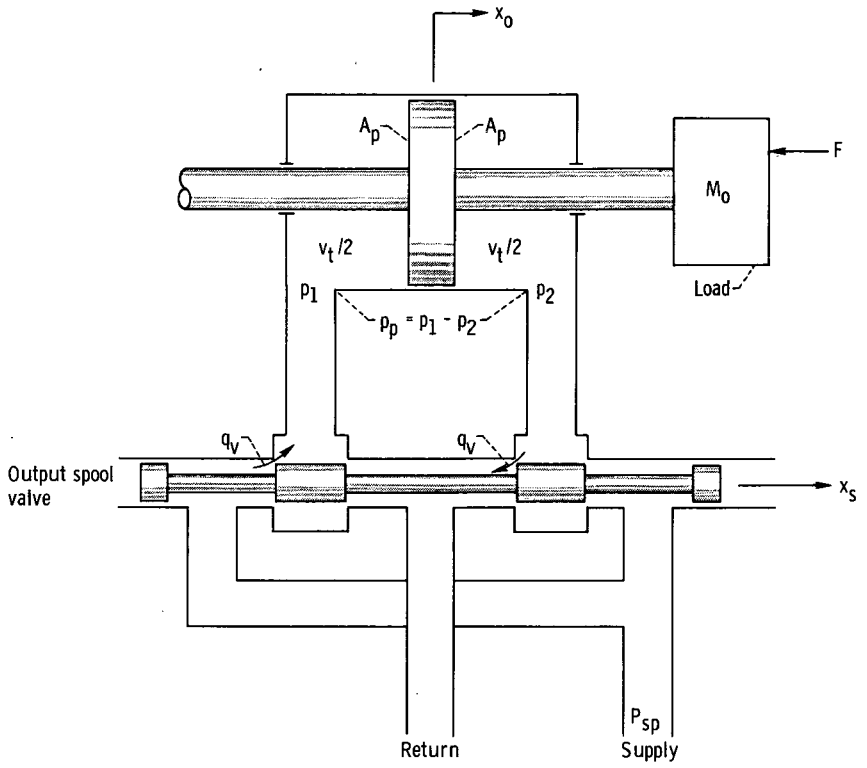

Figure 2. - Schematic representation of servovalve output, piston actuator, and load.

where

$$p_p = p_1 - p_2 \tag{5}$$

Servovalve Output and Actuator Coupling

It is also assumed that the servovalve and piston actuator will be hydraulically closely coupled. There will, however, be some amount of entrapped fluid. For the systems considered, the resonant frequency of the equivalent output mass M_o and this small volume of compressible fluid will occur at frequencies well beyond the range of interest (>100 Hz). Thus, this resonance will not be a limiting factor to system dynamic performance. The equation describing the interconnection of the servovalve and actuator is as follows:

$$q_v(t) = A_p \dot{x}_o(t) + \frac{V_t}{4\beta} \dot{p}_p(t) \tag{6}$$

Equation (6) assumes that the piston is at midposition and that the loads are such that the volumetric flows through each of the spool orifices are equal. Since the entrapped volume is being considered small, the second term on the right side of equation (6) can be neglected. The result is

$$q_v(t) = A_p \dot{x}_o(t) \tag{7}$$

Two-Stage Servovalve

For high-performance servosystems of the type being discussed in this report, a two-stage hydraulic servovalve is employed in almost all cases. This device is shown in detail in figure 3. It employs a spool valve output stage driven by a double jet flapper valve hydraulic preamplifier. This sensitive flapper is driven by the armature of an electromagnetic torque motor. In addition, a force feedback path from the spool to the torque motor armature is included to provide insensitivity to different operating modes. Reference 1 derives the basic relations which describe the operation of this control component. The final describing equations and the assumption upon which they are based will now be presented.

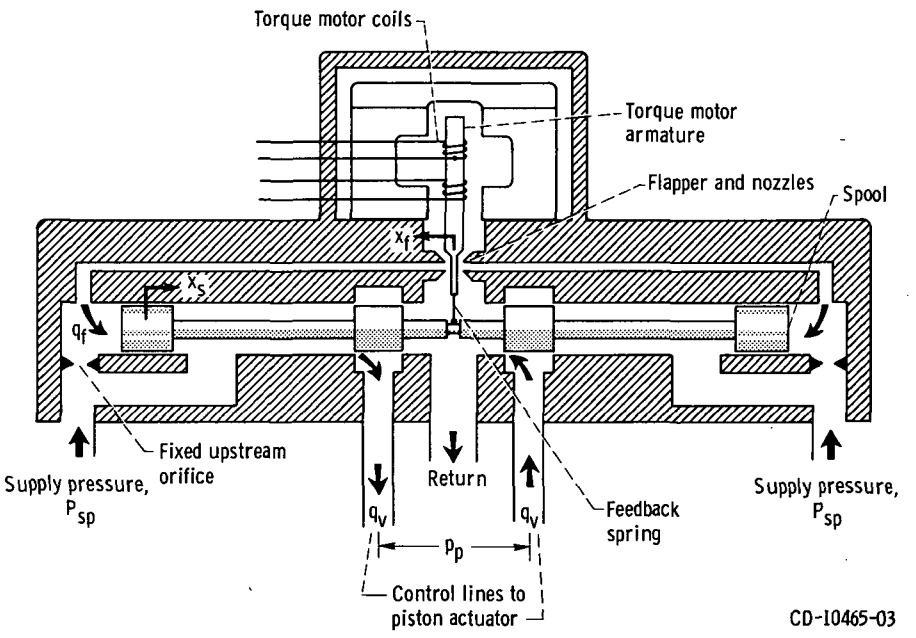

Figure 3. - Schematic representation of two-stage electrohydraulic servovalve.

The servovalve output is supplied as pressure and flow through the spool valve orifices (fig. 2) and through the control lines to the piston actuator. The equation which describes this output as a function of spool displacement x_s is defined by

$$q_v = C_s x_s \sqrt{p_v} \tag{8}$$

where C_s is a lumped coefficient for two identical rectangular orifices in series defined as

$$C_s = C_d w \sqrt{\frac{1}{\rho}} \tag{9}$$

in which

C_d orifice flow coefficient, dimensionless

w width of rectangular orifice, cm

ρ fluid mass density, g/cm^3

and where p_v is the pressure drop across both spool valve orifices in series defined by

$$\left.\begin{aligned} p_v &= P_{sp} - p_p \quad \text{for } x_s > 0 \\ p_v &= P_{sp} + p_p \quad \text{for } x_s < 0 \end{aligned}\right\} \tag{10}$$

in which

$$p_p = p_1 - p_2 \tag{5}$$

and the return pressure is zero. Figure 4 shows the family of valve output characteristics which results from this relation. From this figure, it can be seen that the nonlinear relation between output pressure and flow is physically limited by the maximum spool travel $x_{s,max}$.

The spool displacement is determined by the action of the flapper valve preamplifier. In a well designed servovalve, the pressure forces required to accelerate the spool can be neglected. Thus, the spool motion will be dependent only on the flapper

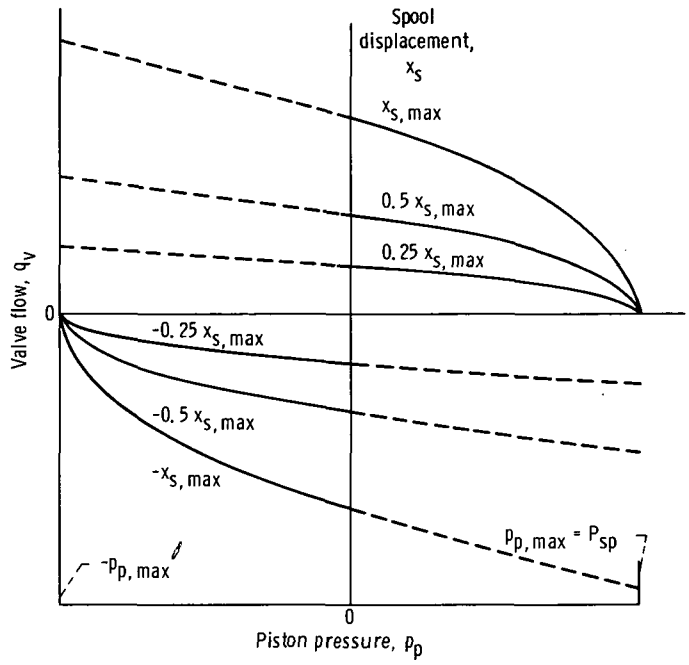

Figure 4. - Generalized servovalve output characteristics.

valve volumetric flow to the spool ends. This action is defined as follows:

$$x_s(t) = \frac{1}{A_s} \int q_f \, dt \tag{11}$$

$$\dot{x}_s(t) = \frac{1}{A_s} q_f(t) \tag{12}$$

As indicated in reference 3, the double jet flapper valve which performs the hydraulic preamplification is an analytically complicated device. Reference 1, however, has investigated this device thoroughly for small flapper displacements. From the results of this work, the flow to the spool from the flapper can be approximated by the following linear relation:

$$q_f = K_{fn} x_f \tag{13}$$

Even though this simple relation is based on many assumptions, previous work in this area (ref. 4) has shown it to be valid in well designed high-performance servovalves.

DISCUSSION OF PERFORMANCE LIMITATIONS

The power required to cause output motion must come directly from the servovalve output stage (spool valve) pressure p_p and flow q_v capabilities. In the past only p_p and q_v have been considered in determining the limitations to the output (load) dynamic performance capabilities. It has been found (ref. 2), however, that in systems operating at higher frequencies flapper valve hydraulic preamplifier stage flow capacity must be considered. Flapper stage flow determines the spool velocity required to supply the power to the load for oscillating motion. At high frequency the required spool velocities become quite high. Inability of the flapper to supply enough flow to permit the required spool velocities will result in peak spool displacements less than $x_{s,max}$. This will prohibit the servovalve from achieving its maximum pressure and flow capability (fig. 4). The section Flapper Flow Limit Criterion will discuss this flapper flow limitation with respect to the spool valve capabilities and load requirements. Criteria will be derived which can be used to select power actuating components that maximize performance.

Maximum Output (Load) Locus

The output or load acceleration can be expressed in terms of the pressure across the piston. Substituting equation (3) into equation (4) and rearranging result in

$$\frac{A_p}{M_o} p_p(t) = -X_o \omega^2 \sin \omega t \tag{14}$$

When equation (7) is used, the output velocity of equation (2) can be expressed in terms of the servovalve output flow as follows:

$$\frac{q_v(t)}{A_p} = X_o \omega \cos \omega t \tag{15}$$

Rearranging equations (14) and (15) results in the following two equations:

$$\frac{q_v(t)}{A_p X_o \omega} = \cos \omega t \tag{16}$$

$$\frac{A_p p_p(t)}{M_o X_o \omega^2} = - \sin \omega t \tag{17}$$

Therefore, for sinusoidal motion of the output $x_o(t)$, equations (16) and (17) show that the servovalve output spool flow $q_v(t)$ and pressure $p_p(t)$ must also be sinusoidal but with a specific phase relation. Figure 5 is a typical plot of the phase relation of the variables $x_o(t)$, $q_v(t)$, and $p_p(t)$. It can be seen that the valve flow $q_v(t)$ leads the output by $\pi/2$ radians and that the flow and pressure are out of phase by $\pi/2$ radians. When the flow and pressure for one complete sine wave are cross plotted on a servovalve characteristic such as figure 4, a load locus will be generated. An expression for this load locus will now be derived.

Squaring both sides of equations (16) and (17) and adding the result yield

$$\frac{q_v^2}{A_p^2 X_o^2 \omega^2} + \frac{A_p^2 p_p^2}{M_o^2 X_o^2 \omega^4} = 1 \tag{18}$$

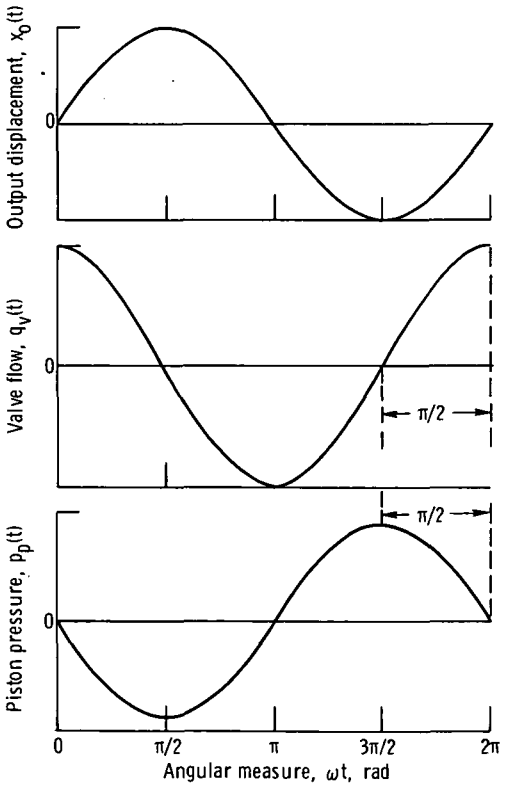

Figure 5. - Typical position, flow, and pressure response during sinusoidal motion.

Equation (18) describes an ellipse and represents the locus that would appear on the servovalve output characteristic of figure 4 for sinusoidal motion of the actuator output position $x_o(t)$.

The largest possible ellipse must be bounded by the maximum spool displacement $\pm x_{s,max}$ and the maximum piston pressures $\pm p_{p,max}$. This region is shown by the outermost boundaries of figure 4. To get the most out of the specialized type of system being discussed in this report, the ellipse described by equation (18) will lie within this region but be tangent to the $\pm x_{s,max}$ curves at some point. The choice of this tangent point is somewhat arbitrary but will be selected to occur at the point of maximum power transfer of the servovalve to the load. This point is designated as point A in figure 6.

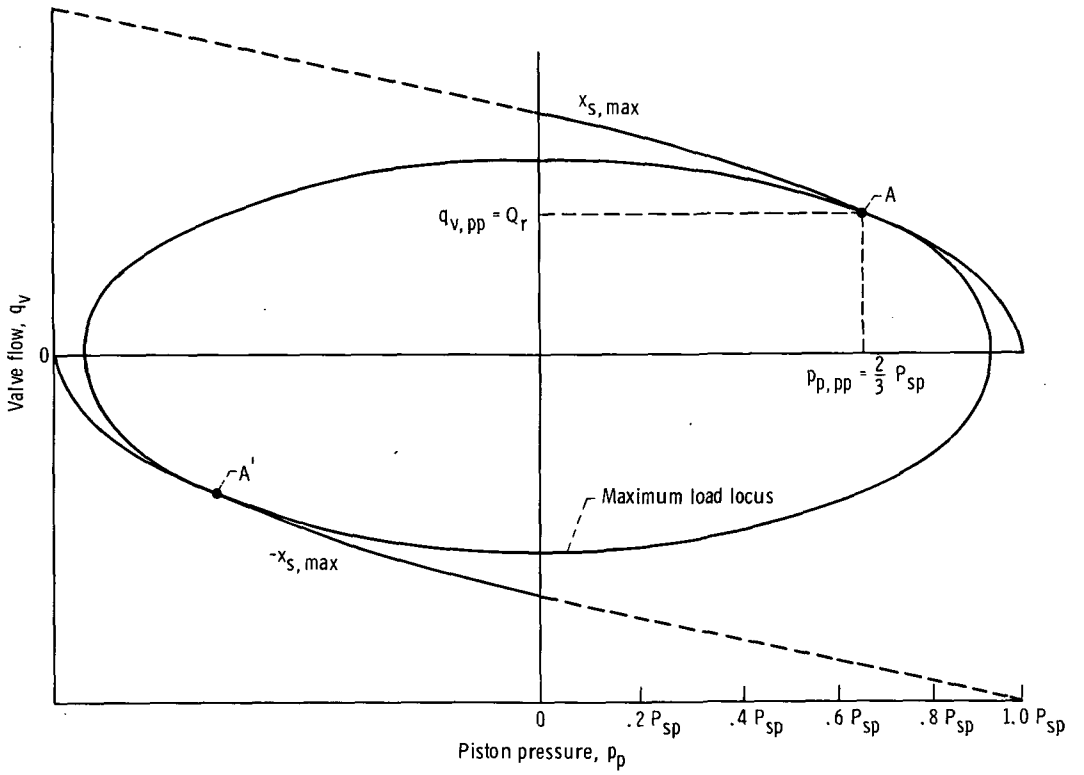

Figure 6. - Servovalve maximum output capabilities and maximum load locus.

The derivation of this point is considered in reference 1, and therefore, only the results will be presented here. The pressure p_p and flow q_v at this peak power point are as follows:

$$p_{p,pp} = \frac{2}{3} P_{sp} \tag{19}$$

$$q_{v,pp} = Q_r \tag{20}$$

where Q_r is defined as the servovalve rated flow that normally appears in the specifications. Rated flow is conventionally defined as the maximum flow available from the valve with $(2/3)P_{sp}$ across the load.

The derivation of the equation for the load locus or ellipse which is tangent to the $x_{s,max}$ curve at point A of figure 6 can be found in appendix B. The result is repeated here:

$$\frac{q_v^2}{2Q_r^2} + p_p^2\left(\frac{9}{8P_{sp}^2}\right) = 1 \tag{21}$$

A plot of this load locus is presented in figure 6 as the ellipse passing through point A. In terms of supply pressure P_{sp} and rated flow Q_r, its intercepts with the p_p and q_v axes are as follows:

$$p_{p,peak} = \frac{2}{3}\sqrt{2}\,P_{sp} \tag{22}$$

$$q_{v,peak} = \sqrt{2}\,Q_r \tag{23}$$

These are the peak piston pressure and flow values which the servovalve must supply to enable the output load to generate the locus of equation (21) when operating in a sinusoidal manner. The values of peak pressure and flow defined by equations (22) and (23) then determine the output acceleration and velocity limit criteria, respectively.

Acceleration and Velocity Limit Criteria

To derive an expression for the output acceleration limit only peak values of equation (14) are considered, and the following equation is obtained:

$$\frac{A_p}{M_o}\,p_{p,peak} = X_o\omega^2 \tag{24}$$

Substituting $p_{p,peak}$ from equation (22) into equation (24) results in the expression for the output acceleration limit criterion:

$$X_o\omega^2 = \frac{A_p}{M_o}\frac{2}{3}\sqrt{2}\,P_{sp} \tag{25}$$

To derive an expression for the output or load velocity limit, only peak values of equation (15) are considered, and the result is

$$\frac{q_{v,peak}}{A_p} = X_o\omega \tag{26}$$

Substituting $q_{v,peak}$ from equation (23) into equation (26) gives the expression for the output velocity limit criterion:

$$X_o\omega = \frac{\sqrt{2}\,Q_r}{A_p} \tag{27}$$

Flapper Flow Limit Criterion

Reference 2 notes that for fast-response (>100 Hz) actuation systems with primarily inertia-type loads, the flow capacity of the flapper valve hydraulic preamplifier (see fig. 3) must be a consideration in determining output performance limitations. An expression defining this limitation in terms of the output characteristics will now be derived.

It should be remembered that sinusoidal motion of the output shaft as defined by equation (15), and repeated here for clarity,

$$\frac{q_v(t)}{A_p} = X_o\omega\cos\omega t \tag{15}$$

requires displacement and velocity of the servovalve spool. The relation between flow q_v and spool displacement x_s is from equation (8):

$$q_v = C_s x_s\sqrt{p_v}$$

This is not a linear relation. Therefore, when the output is operating sinusoidally and generating the maximum locus of figure 6, the nonlinear relation of equation (8) prohibits the spool displacement from being sinusoidal. The solid curve of figure 7 is a

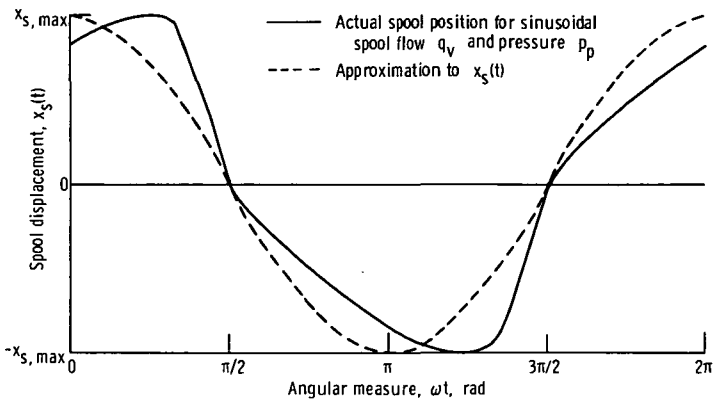

Figure 7. - Response of spool position required for sinusoidal piston motion.

plot of the spool displacement as a function of time under these conditions. It can be seen that the peak values required are $\pm x_{s,max}$ as would be expected since the output ellipse (fig. 6) is tangent to these curves at points A and A'. An assumption, however, is now made that this distorted waveform (solid curve of fig. 7) can be approximated by a sinusoidal waveform (dashed curve) of the same peak amplitude. If this is done, the spool displacement $x_s(t)$ and spool flow $q_v(t)$ can be related as follows:

$$x_s(t) = K_s q_v(t) \tag{28}$$

or

$$x_{s,max} \cos(\omega t + \varphi) = K_s q_{v,peak} \cos(\omega t + \varphi) \tag{28a}$$

When equation (23) is used and only peak values are considered, equation (28a) yields $K_s = x_{s,max}/(\sqrt{2}\, Q_r)$. Thus, equation (28) becomes

$$x_s(t) = \frac{x_{s,max}}{\sqrt{2}\, Q_r} q_v(t) \tag{29}$$

When the expression for $q_v(t)$ from equation (7) is used, equation (29) becomes

$$x_s(t) = \frac{x_{s,max}}{\sqrt{2}\, Q_r} A_p \dot{x}_o(t) = \frac{x_{s,max}}{\sqrt{2}\, Q_r} A_p X_o \omega \cos \omega t \tag{30}$$

Differentiation yields

$$\dot{x}_s(t) = -A_p \frac{x_{s,max}}{\sqrt{2}\, Q_r} X_o \omega^2 \sin \omega t \tag{31}$$

From equation (12) the spool velocity can be expressed in terms of the flapper valve flow $q_f(t)$. Substituting equation (12) into equation (31) and rearranging yields:

$$q_f(t) = -A_s A_p \frac{x_{s,max}}{\sqrt{2}\, Q_r} X_o \omega^2 \sin \omega t \tag{32}$$

If only the peak values of $q_f(t)$ are considered, rearrangement of equation (32) results in the flapper flow limit criterion:

$$X_o \omega^2 = \frac{\sqrt{2}\, Q_r q_{f,max}}{A_p A_s x_{s,max}} \tag{33}$$

Note that the value for $q_{f,max}$ will not be the same as that given by equation (13) when $x_{f,max}$ and K_{fn} are used. This is due to the nonlinearity of the flapper valve for large motions. The maximum flapper flow $q_{f,max}$ must be determined empirically and is generally greater than the product of K_{fn} and $x_{f,max}$.

LIMIT CRITERIA FOR REGION OF MAXIMUM DYNAMIC PERFORMANCE CAPABILITY

The three limiting relations defined by equations (27), (25), and (33) are repeated here for clarity:

Velocity limit

$$X_o \omega = \frac{\sqrt{2}\, Q_r}{A_p} \tag{27}$$

Acceleration limit

$$X_o \omega^2 = \frac{\frac{2}{3}\sqrt{2}\, P_{sp} A_p}{M_o} \tag{25}$$

Flapper flow limit

$$X_o\omega^2 = \frac{\sqrt{2}\, Q_r q_{f,\max}}{A_p A_s x_{s,\max}} \tag{33}$$

For a specific application in which the load mass and the supply pressure available are specified, these criteria are all a function of the piston actuator area and the capacity of specific servovalves. For a particular servovalve, the curves will depend only on piston area. Figure 8 is presented to show the generalized displacement or shift of

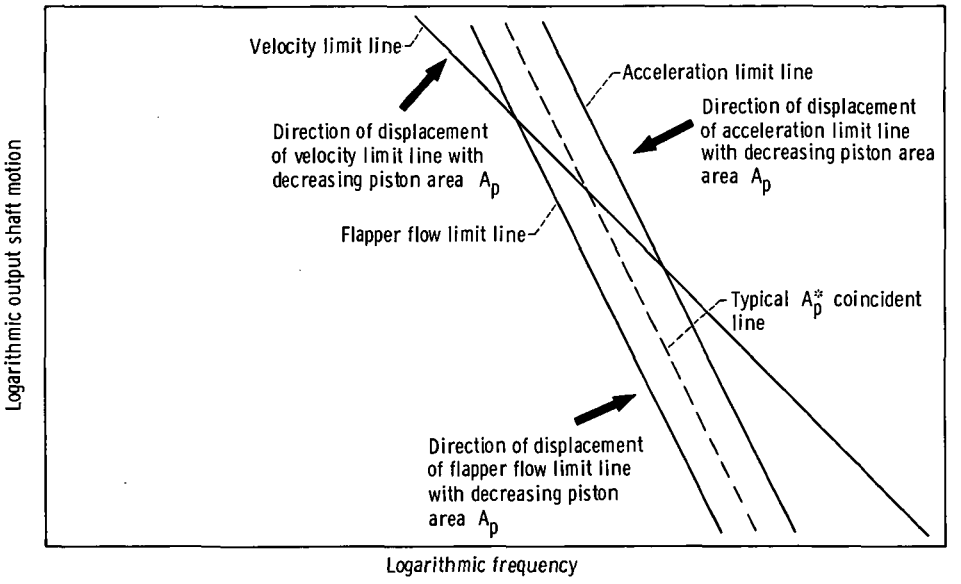

Figure 8. - General limit lines showing dependence on piston area.

each limit line as a function of piston area. It can be seen from this figure that for a specific value of piston area A_p the parallel flapper flow line and output acceleration line can be made to coincide. The piston area at which this coincidence occurs can be determined as follows. Setting equation (25) equal to (33) yields

$$\frac{\sqrt{2}\, Q_r q_{f,\max}}{A_p A_s x_{s,\max}} = \frac{\frac{2}{3}\sqrt{2}\, P_{sp} A_p}{M_o} \tag{34}$$

Solving for the coincident piston area yields

$$A_p^* = \sqrt{\frac{M_o Q_r q_{f,\max}}{\frac{2}{3} P_{sp} A_s x_{s,\max}}} \tag{35}$$

The area A_p^* is defined as the "optimum" piston area for the type of actuation servosystems being considered in this analysis. Use of A_p^* will maximize the high-frequency region of dynamic performance capability. An example of the use of these three limit lines of equation (25), (27), and (33) and the "optimum" piston area A_p^* of equation (35) is presented in the next section.

APPLICATION OF LIMIT CRITERIA

The limit criteria were applied to an actual experimental system actuated by an electrohydraulic servosystem like that of figure 4. The system was an overboard bypass valve for an experimental supersonic inlet and was designed for fast-response operation. The bypass valve and servosystem are shown in figure 9. The bypass valve

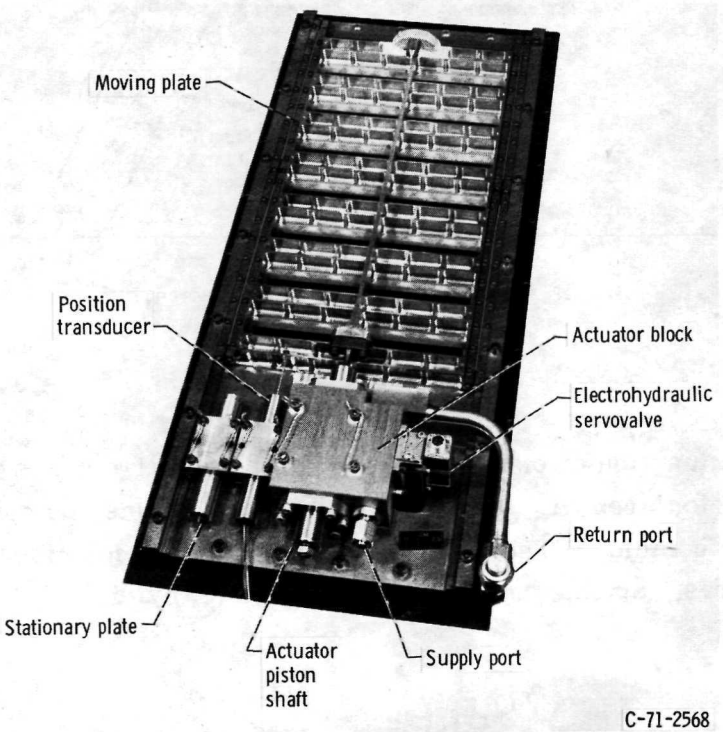

Figure 9. - Slotted-plate overboard bypass valve and servosystem.

servosystem can be used for studying propulsion system dynamics, or it can be incorporated into a control loop for controlling the inlet terminal shock position. The valve portion consists of two slotted plates with the stationary bottom plate used as a base for mounting the actuator and position transducer. This is more clearly illustrated in the section drawing of figure 10. The top plate moves on roller bearings with a motion parallel to the stationary plate. This motion varies the airflow area of the valve. The servoactuator is used to position the moving plate and thus controls the airflow area.

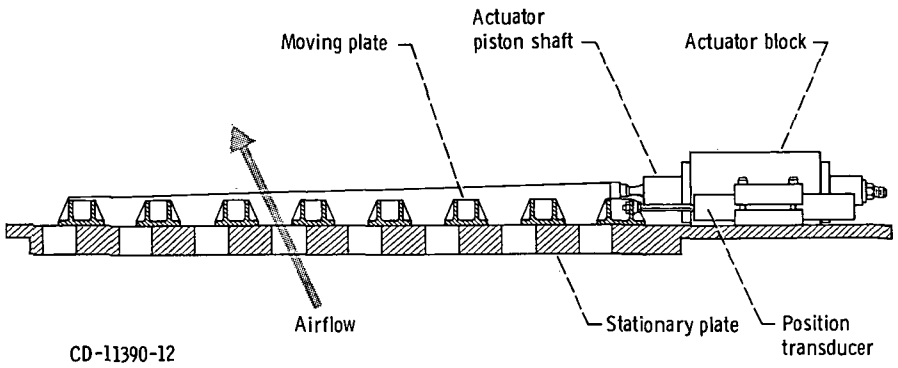

Figure 10. - Section view of slotted-plate overboard bypass valve.

The position transducer provides a feedback signal for closed-loop control, as shown in figure 1. This system provides a valve position output proportional to the command voltage input.

The dynamic performance of this servosystem can be predicted by using equations (27), (25), and (33). The parameters which are characteristic of the bypass valve servosystem are presented in table I. From these data the limit equations are as follows:

Velocity limit

$$X_0\omega = 2.77\times10^2 \text{ cm/sec} \tag{36}$$

Acceleration limit

$$X_0\omega^2 = 1.28\times10^5 \text{ cm/sec}^2 \tag{37}$$

Flapper flow limit

$$X_0\omega^2 = 1.04\times10^5 \text{ cm/sec}^2 \tag{38}$$

TABLE I. - BYPASS VALVE SERVOSYS-

TEM PHYSICAL CONSTANTS

Piston area, A_p, cm^2	2.58
Spool area, A_s, cm^2	0.342
Output mass, M_o, kg	3.94
Supply pressure, P_{sp}, N/cm^2	2070
Rated volumetric flow, Q_r, cm^3/sec	505
Maximum flapper volumetric flow, $q_{f,max}$, cm^3/sec	5.74
Maximum spool linear displacement $x_{s,max}$, cm	0.0445

The limit lines described by these equations are plotted in figure 11. For large-amplitude displacements the response is limited by the velocity limit, whereas for smaller displacements the system response is limited by the flapper flow limit line. For this servosystem the intersection of these limit lines occurs at a frequency of 60 hertz and a zero-to-peak displacement of 0.74 centimeter.

The optimum piston area for this system will be 2.34 square centimeters if equation (35) and table I are used. The actual piston area listed in table I is 2.58 square

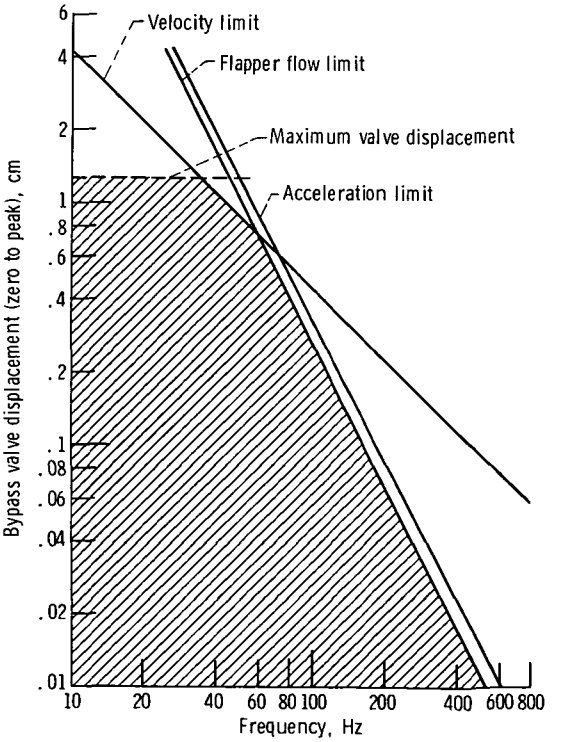

Figure 11. - Region of dynamic performance for bypass valve.

centimeters, which is close to optimum. (The use of standard size components prohibited the exact selection of the optimum area.) This can be seen in figure 11 from the fact that the acceleration and flapper flow limit lines are close to each other. Had the piston area been optimum, these lines would have coincided.

The dynamic response measured experimentally with the bypass valve servosystem is plotted in figure 12 along with the two limit lines which predict performance. These lines coincide with the experimental data and verify the validity of the limit relations as a means of predicting dynamic performance capability.

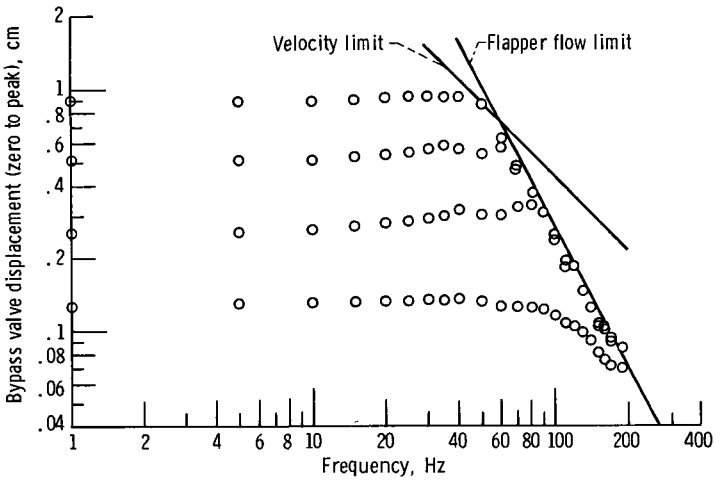

Figure 12. - Experimental position response of bypass valve with limit lines superimposed.

GENERALIZED DESIGN CRITERION USING LIMIT CRITERIA

Figure 8 shows that the boundary of dynamic performance capabilities consists of two straight lines which intersect at a common point. For the optimized piston area case, they are the piston velocity and coincident flapper flow and piston acceleration limit lines. It should be noted that the piston velocity limit line has a slope of -1 on the logarithmic plot, while the flapper flow or piston acceleration limit lines have a slope of -2. The intersection point or "corner point" from which these lines emanate has associated with it displacement and frequency coordinates, which will be defined as X_o^{**} and ω^{**}, respectively.

From the direction of the flapper flow limit line shown in figure 8 for decreasing piston area (to the right), it can be seen that the corner point (X_o^{**}, ω^{**}) for all piston areas greater than or equal to A_p^* will be determined by the intersection of the piston velocity and flapper flow limit lines. The relation for these coordinates can be determined as follows. Substituting equation (27) into equation (33) and solving for ω^{**} result in

$$\omega^{**} = \frac{q_{f,\max}}{A_s x_{s,\max}} \tag{39}$$

for $A_p \geq A_p^*$. Substituting this expression for ω^{**} in equation (27) and solving for X_o^{**} yield

$$X_o^{**} = \frac{\sqrt{2}\, Q_r A_s x_{s,\max}}{A_p q_{f,\max}} \tag{40}$$

for $A_p \geq A_p^*$.

For piston areas smaller than A_p^*, a review of figure 8 will show that the piston acceleration limit line will lie to the left of the flapper flow limit line. Thus, for the case $A_p < A_p^*$ the point of intersection (X_o^{**}, ω^{**}) for the boundary of dynamic performance capability will be determined by the piston acceleration and velocity limit lines. Relations for the coordinates X_o^{**} and ω^{**} can be determined as follows. Substituting equation (27) into equation (25) and solving for ω^{**} yield

$$\omega^{**} = \frac{\frac{2}{3} P_{sp} A_p^2}{Q_r M_o} \tag{41}$$

for $A_p < A_p^*$. Substituting equation (41) into equation (27) and solving for X_o^{**} yield

$$X_o^{**} = \frac{\sqrt{2}\, Q_r^2 M_o}{A_p^3 \frac{2}{3} P_{sp}} \tag{42}$$

for $A_p < A_p^*$.

Figure 13 shows the locus of the point of intersection (X_o^{**}, ω^{**}) for various piston areas. The coordinates have been normalized to the point of intersection at the optimum area A_p^*. The coordinates for this normalizing point are ω^*, X_o^*.

The locus for piston areas greater than A_p^* is determined by equations (39) and (40). Since the frequency ω^{**} defined by equation (39) is not a function of the piston area A_p, the locus for $A_p > A_p^*$ is the vertical line shown in figure 13.

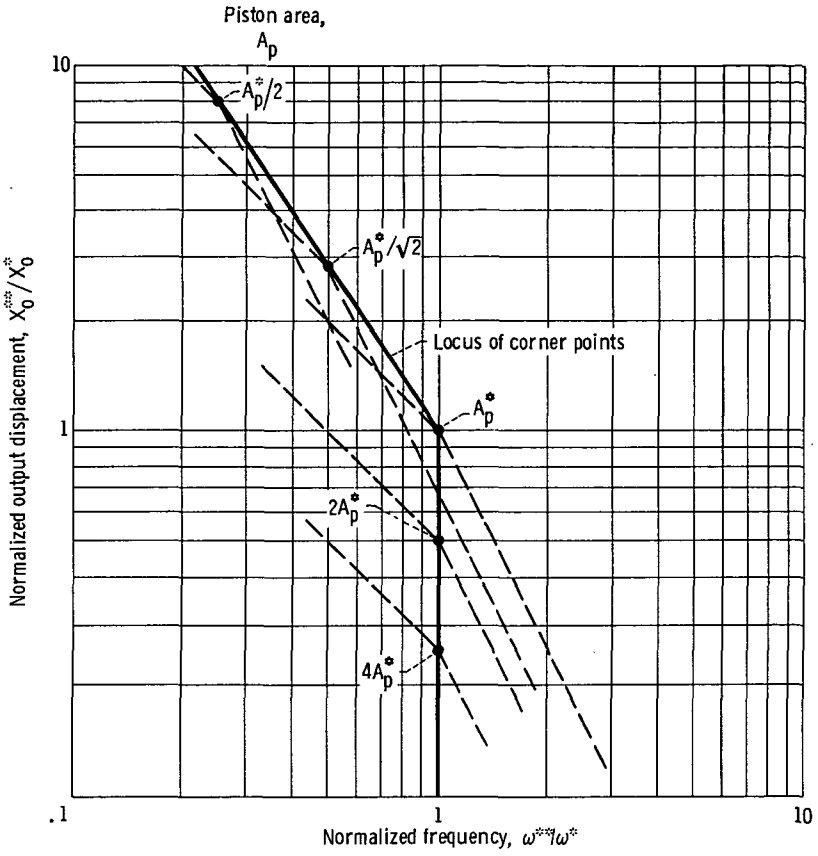

Figure 13. - Locus of normalized corner points for region of dynamic performance capabilities.

If the piston area A_p is less than the optimum area A_p^*, the locus may be determined from equations (41) and (42). These two equations imply that

$$X_o^{**} \alpha \omega^{-3/2}$$

for $A_p < A_p^*$. Hence, the locus of figure 13 has a slope of -3/2 for $A_p < A_p^*$.

Knowledge of the coordinates at $A_p = A_p^*$ therefore is sufficient to determine the corner point locus completely. For this reason, the locus of figure 13 has been normalized to the coordinates at this point. The coordinates at $A_p = A_p^*$ (X_o^*, ω^*) are defined by

$$X_o^* = \frac{\sqrt{2}\, Q_r A_s x_{s,\max}}{A_p^* q_{f,\max}} \tag{43}$$

$$\omega^* = \frac{q_{f,\max}}{A_s x_{s,\max}} \tag{44}$$

where

$$A_p^* = \sqrt{\frac{M_o Q_r q_{f,\max}}{\frac{2}{3} P_{sp} A_s x_{s,\max}}} \tag{35}$$

The ratio of piston areas A_p/A_p^* determines where the corner point is on the normalized locus of figure 13. From equations (39) to (44), the following relations can be derived:

For $A_p > A_p^*$

$$\frac{X_o^{**}}{X_o^*} = \frac{A_p^*}{A_p} < 1 \tag{45}$$

$$\frac{\omega^{**}}{\omega^*} = 1 \tag{46}$$

For $A_p < A_p^*$

$$\frac{X_o^{**}}{X_o^*} = \left(\frac{A_p^*}{A_p}\right)^3 > 1 \tag{47}$$

$$\frac{\omega^{**}}{\omega^*} = \left(\frac{A_p}{A_p^*}\right)^2 < 1 \tag{48}$$

Thus, equations (35) and (43) to (48) completely describe the position of the corner point. On the normalized plot of figure 13 also are included several boundary lines which emanate from the corner points. The velocity limit has a slope of -1 to the left, and the flapper flow or acceleration limits have a slope of -2 to the right.

With this rather complete picture of the possible regions of dynamic performance capability, a few observations should be made. For piston areas greater than the opti-

mum A_p^*, the boundary lines move to the left and actually decrease the region of dynamic performance capability. Thus, unless the requirements of the opposing force loads demand the larger piston areas, A_p^* will result in the highest frequency-amplitude performance.

For piston areas smaller than A_p^*, figure 13 shows that high-frequency performance is sacrificed to gain lower frequency operation at larger amplitudes of X_o.

CONCLUDING REMARKS

A detailed analysis has been made of the nonlinear and limiting aspects of the power actuation components of electrohydraulic actuation servosystems for high-response (>100 Hz) research applications. The analysis has considered the major load to be inertial (mass) and has assumed the actuator to be closely coupled to the valve. The maximum capacities of the servovalve spool valve have been considered in the analysis. The spool limitations for flow and pressure to the piston as well as the flow capacity of the flapper valve preamplifier have been used to derive limit criteria. These criteria have been applied to the experimental performance of a fast-response actuation system. The correlation of the experimental results with the predicted limit region is excellent.

The limit criteria will define a maximum region of dynamic performance capability for a particular system. Classical linear control design techniques can then be employed to ensure stable dynamic performance throughout this region of capability. In addition, the improved limit criteria have been used to formulate a generalized design criterion for selecting power actuation components.

Lewis Research Center,
National Aeronautics and Space Administration,
Cleveland, Ohio, November 30, 1972,
501-24.

APPENDIX A

SYMBOLS

A	area, cm^2
C	coefficient (nonlinear)
F	force, N
K	coefficient (linearized)
M	mass, $(N)(sec^2)/cm$
P	pressure (steady-state), N/cm^2
p	pressure (instantaneous), N/cm^2
Q	volumetric flow (steady-state), cm^3/sec
q	volumetric flow (instantaneous), cm^3/sec
t	time, sec
V	volume, cm^3
X	linear displacement (peak of sine wave), cm
x	linear displacement (instantaneous), cm
β	bulk modulus, N/cm^2
φ	phase angle, rad
ω	frequency, rad/sec

Subscripts:

A	peak power point
f	flapper
fn	flapper nozzle
max	maximum
o	output
p	piston
peak	peak
pp	peak power
r	rated

s	spool
sp	supply pressure
t	total
v	valve
1, 2	left and right side of piston

Superscripts:

( )*	optimum
( )**	corner point
$\dot{(\ )}$	first derivative with respect to time
$\ddot{(\ )}$	second derivative with respect to time

APPENDIX B

DERIVATION OF RELATION OF MAXIMUM OUTPUT PRESSURE TO FLOW LOCUS

From equations (8) and (9) the expression for the servovalve pressure-flow characteristic at maximum spool displacement $x_{s,max}$ is as follows:

$$q_v = C_s x_{s,max} \sqrt{P_{sp} - p_p} \tag{B1}$$

The generalized expression for the pressure and flow output requirements during sinusoidal output motion is given by equation (18). After rearranging, this equation becomes

$$q_v^2 = \omega^2 X_o^2 A_p^2 - p_p^2 \left(\frac{A_p^4}{M_o^2 \omega^2} \right) \tag{B2}$$

To determine a specific expression of the load ellipse that is tangent to the servovalve characteristic at point A (fig. 5), the derivatives dq_v/dp_p of equations (B1) and (B2) are determined and equated. The result is

$$\frac{-C_s x_{s,max}}{2\sqrt{P_{sp} - p_p}} = -\frac{p_p}{q_v} \left(\frac{A_p^2}{M_o^2 \omega^2} \right) \tag{B3}$$

Substituting $q_v = C_s x_{s,max} \sqrt{P_{sp} - p_p}$ and rearranging give

$$\frac{q_v}{2(P_{sp} - p_p)} = \frac{p_p}{q_v} \left(\frac{A_p^4}{M_o^2 \omega^2} \right) \tag{B4}$$

Substituting in the coordinates of point A of figure 5 ($(2/3)P_{sp}$, Qr) yields an expression for ω_A, the frequency of oscillation for the output locus which passes through point A:

$$\omega_A = \frac{\frac{2}{3} P_{sp} A_p^2}{M_o Q_r} \tag{B5}$$

Substituting equation (B5) into equation (B2) at the coordinates of point A yields the peak displacement $X_{o,A}$ for the locus through point A:

$$X_{o,A} = \frac{3\sqrt{2}\, Q_r^2 M_o}{2A_p^3 P_{sp}} \tag{B6}$$

Substitution of equations (B5) and (B6) into the general expression of equation (B2) yields the expression for the maximum output (load) pressure and flow locus:

$$q_v^2 = 2Q_r^2 - p_p^2\left(\frac{9}{4}\frac{Q_r^2}{P_{sp}^2}\right) \tag{B7}$$

Rearranging yields the following:

$$\frac{q_v^2}{2Q_r^2} + p_p^2\left(\frac{9}{8P_{sp}^2}\right) = 1 \tag{B8}$$

This is the expression used in the main text for derivation of the output performance limit criteria.

REFERENCES

1. Merrit, Herbert E.: Hydraulic Control Systems. John Wiley & Sons, Inc., 1967.
2. Zeller, John R.: Analysis of Dynamic Performance Limitations of Fast Response (150 to 200 Hz) Electrohydraulic Servos. NASA TN D-5388, 1969.
3. Shashkov, A. G.: Theory of Control Devices of the "Nozzle Baffle" Type, Working with Oil. Pneumatic and Hydraulic Control Systems. Vol. 1. M. A. Aizerman, ed. (P. Linnik, trans.), Pergamon Press, 1968, pp. 285-308.
4. Thayer, W. J.: Transfer Functions for Moog Servovalves. Tech. Bull. No. 103, Moog Servocontrols, Inc., Jan. 1965.

NASA-Langley, 1973 — 3 E-7239

NATIONAL AERONAUTICS AND SPACE ADMINISTRATION
WASHINGTON, D.C. 20546

OFFICIAL BUSINESS
PENALTY FOR PRIVATE USE $300

SPECIAL FOURTH-CLASS RATE BOOK

POSTAGE AND FEES PAID
NATIONAL AERONAUTICS AND SPACE ADMINISTRATION
451

U.S.MAIL

POSTMASTER: If Undeliverable (Section 158 Postal Manual) Do Not Return

"The aeronautical and space activities of the United States shall be conducted so as to contribute . . . to the expansion of human knowledge of phenomena in the atmosphere and space. The Administration shall provide for the widest practicable and appropriate dissemination of information concerning its activities and the results thereof."

—NATIONAL AERONAUTICS AND SPACE ACT OF 1958

NASA SCIENTIFIC AND TECHNICAL PUBLICATIONS

TECHNICAL REPORTS: Scientific and technical information considered important, complete, and a lasting contribution to existing knowledge.

TECHNICAL NOTES: Information less broad in scope but nevertheless of importance as a contribution to existing knowledge.

TECHNICAL MEMORANDUMS: Information receiving limited distribution because of preliminary data, security classification, or other reasons. Also includes conference proceedings with either limited or unlimited distribution.

CONTRACTOR REPORTS: Scientific and technical information generated under a NASA contract or grant and considered an important contribution to existing knowledge.

TECHNICAL TRANSLATIONS: Information published in a foreign language considered to merit NASA distribution in English.

SPECIAL PUBLICATIONS: Information derived from or of value to NASA activities. Publications include final reports of major projects, monographs, data compilations, handbooks, sourcebooks, and special bibliographies.

TECHNOLOGY UTILIZATION PUBLICATIONS: Information on technology used by NASA that may be of particular interest in commercial and other non-aerospace applications. Publications include Tech Briefs, Technology Utilization Reports and Technology Surveys.

Details on the availability of these publications may be obtained from:

SCIENTIFIC AND TECHNICAL INFORMATION OFFICE

NATIONAL AERONAUTICS AND SPACE ADMINISTRATION

Washington, D.C. 20546